Study of a control strategy for grid side converter in doubly-fed wind power system

D J Zhu, Z L Tan[1], F Yuan, Q Y Wang and M Ding

School of Automation, China University of Geosciences, No. 388 Lumo Road, Wuhan, China

E-mail: tanzhili@cug.edu.cn

Abstract. The grid side converter is an important part of the excitation system of doubly-fed asynchronous generator used in wind power system. As a three-phase voltage source PWM converter, it can not only transfer slip power in the form of active power, but also adjust the reactive power of the grid. This paper proposed a control approach for improving its performance. In this control approach, the dc voltage is regulated by a sliding mode variable structure control scheme and current by a variable structure controller based on the input output linearization. The theoretical bases of the sliding mode variable structure control were introduced, and the stability proof was presented. Switching function of the system has been deduced, sliding mode voltage controller model has been established, and the output of the outer voltage loop is the instruction of the inner current loop. Affine nonlinear model of two input two output equations on d-q axis for current has been established its meeting conditions of exact linearization were proved. In order to improve the anti-jamming capability of the system, a variable structure control was added in the current controller, the control law was deduced. The dual-loop control with sliding mode control in outer voltage loop and linearization variable structure control in inner current loop was proposed. Simulation results demonstrate the effectiveness of the proposed control strategy even during the dc reference voltage and system load variation.

1. Introduction

Doubly-fed induction generator is one of the currently widely used in variable speed constant frequency (VSCF) wind power generation system. Its excitation system composed of the rotor side converter and grid side converter. When the wind speed changes caused by generator speed, by controlling the frequency of the rotor current, can make the output frequency constant on stator side. Due to the variable speed constant frequency control scheme are implemented by the rotor circuit, the slip power is only a small part of the generator rated power, so the capacity of converter for the excitation system is small with low voltage. In addition, the excitation control can adjust the amplitude of the excitation current, frequency, phase and phase sequence, so the doubly-fed induction generator with rotor excitation can control of active and reactive power flexibly, which means that it can compensate the reactive power for grid. As an important part of the excitation system of doubly-fed asynchronous generator, the grid side converter can not only transfer slip power in the form of active

[1] Address for correspondence: Z L Tan, School of Automation, China University of Geosciences, No. 388 Lumo Road, Wuhan, China. E-mail: tanzhili@cug.edu.cn.

power, but also adjust the reactive power of the grid, which means that the wind power system has reactive power adjustment ability. The grid side converter couples with the rotor side converter by the dc bus capacitance, the doubly-fed induction generator can be normal excited and good running characteristics, directly related to dynamic and static characteristics of it, so its performance has effect on the efficiency and stability of power system [1, 2].

The grid side converter is a three-phase voltage source PWM converter, the common control methods for which include: PID controller and its improvement method[3,4], Fast adaptive control [5], Model Predictive Current Control [6] ,Dead-Beat control [7,8], one-cycle control [9], intelligent control methods such as neural network [10], Hamiltonian control[11], etc. These control methods have their advantages respectively, but at the same time they have poor adaptability and is difficult to realize coordinated control. Sliding mode control (SMC) is a kind of effective nonlinear control method. It has strong robustness and implement simply, suitable for controlling nonlinear three-phase voltage source PWM converter. This paper aims at the control strategy for the grid side converter , a double-closed-loop control strategy is proposed, which includes outer voltage loop based on sliding mode variable structure control and inner current loop based on variable structure with input-output linearization control strategy .The simulation results prove its validity.

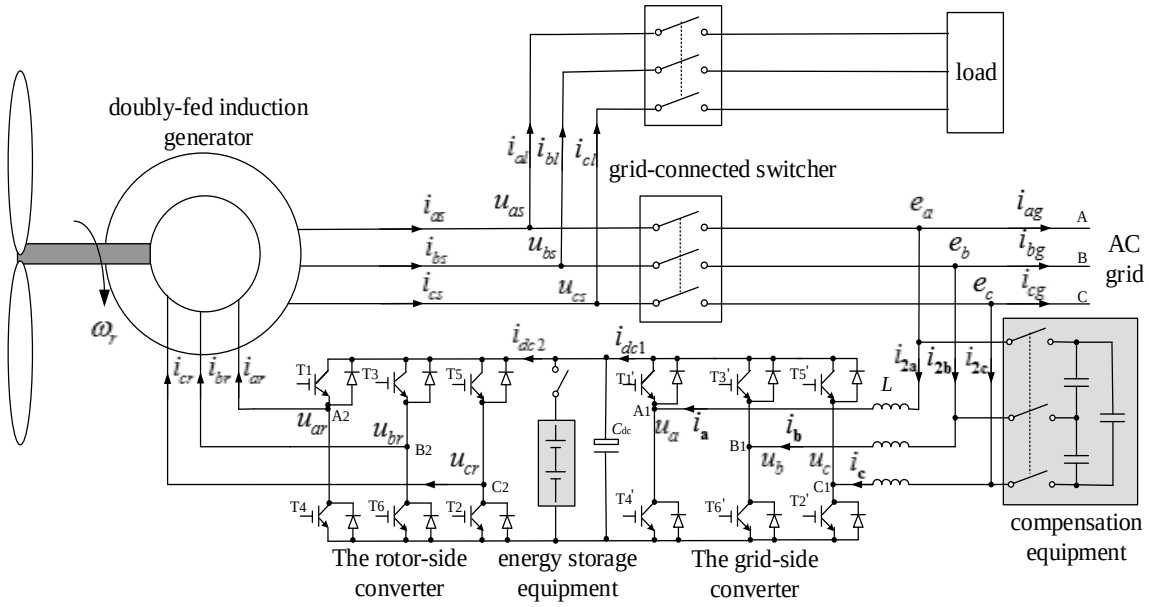

Figure 1. Doubly-fed induction generation in wind power system

2. The mathematical model of grid side converter

From the perspective of the grid side converter, the rotor side converter and dc capacitance can be considered as its loads. The grid side converter is a three-phase voltage source PWM rectifier [2]. Defined the switch function is

$$S_k = \begin{cases} 1 & \text{the upper bridge arm is on and the lower off} \\ 0 & \text{the upper bridge arm is off and the lower on} \end{cases} \quad (k = a,b,c) \tag{1}$$

According to the Kirchhoff's voltage law, the circuit equation for each phase of the three-phase PWM converter is

$$L\frac{di_k}{dt} + R_L i_k = e_k - u_k \quad (k = a,b,c) \tag{2}$$

In addition, using the Kirchhoff's current law on the positive node on the dc side capacitor, we get the Equation (3).

$$C\frac{dU_{dc}}{dt} = i_a S_a + i_b S_b + i_c S_c - i_{dc2} \tag{3}$$

Choose the d axis is consistent with the grid voltage vector $\boldsymbol{E}$, namely $e_d = E$, $e_q = 0$. The grid side converter mathematical model on d-q axis can be transformed from the three-phase static coordinate described as in Equation (2) and (3).

$$\begin{cases} L\dfrac{di_d}{dt} = -R_L i_d + \omega L i_q - u_d + e_d \\ L\dfrac{di_q}{dt} = -R_L i_q - \omega L i_d - u_q \end{cases} \tag{4}$$

$$C\frac{dU_{dc}}{dt} = S_d i_d + S_q i_q - i_{dc2} \tag{5}$$

The equivalent circuit of the grid side converter on d-q axis is shown in figure 2.

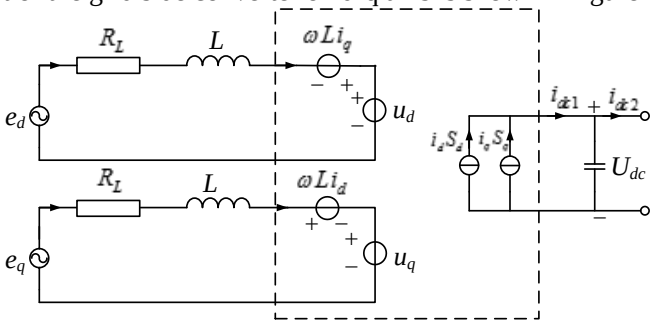

Figure 2. The equivalent circuit of the grid side converter on d-q axis

3. The voltage loop based on sliding mode variable structure control

It can be seen that the grid side converter is a mutual coupling nonlinear time-varying systems from the figure 2, so the conventional linear control strategy is difficult to achieve satisfactory control effect in the aspect of dynamic characteristics and robustness [5]. Therefore, to design a controller voltage with fast dynamic response and robustness for grid side converter, without relying on the switch devices and load parameters, the sliding mode variable structure control is definitely a good choice.

If the loss of inductance and resistance on ac side of the converter are ignored, equation (5) is multiplied by U_{dc} on both sides and then the output power on the dc side P can be obtained by:

$$P = u_d i_d + u_q i_q = (C\frac{dU_{dc}}{dt} + i_{dc2})U_{dc} = (S_d i_d + S_q i_q)U_{dc} \tag{6}$$

so

$$\begin{cases} S_d = u_d / U_{dc} \\ S_q = u_q / U_{dc} \end{cases} \tag{7}$$

Under the steady state conditions, ignoring the ac resistance R_L in equation (4), and considering that $di_d/dt = di_q/dt = 0$, u_d and u_q can be got from equation (4), as shown in equation (8)

$$\begin{cases} u_d = e_d + \omega L i_q \\ u_q = -\omega L i_d \end{cases} \tag{8}$$

Let $e_i = i_q^* - i_q$, $e_u = U_{dc}^* - U_{dc}$, define two sliding surfaces described by

$$\begin{cases} \sigma_i = c_1 e_i + \dot{e}_i \\ \sigma_u = c_2 e_u + \dot{e}_u \end{cases} \tag{9}$$

Where $\dot{e}_i$ and $\dot{e}_u$ are their derivative respectively, and c_1 and c_2 are positive constants.

To prove the stability of the proposed SM at the origin ($\sigma_i = 0$ and $\sigma_u = 0$), let the Lyapunov candidate be

$$\begin{cases} V(e_i) = \frac{1}{2} e_i^2 \\ V(e_u) = \frac{1}{2} e_u^2 \end{cases} \tag{10}$$

Therefore, its time derivative can be expressed as

$$\begin{cases} \dot{V}(e_i) = e_i \dot{e}_i = e_i(-c_1 e_i) = -c_1 e_i^2 < 0 \\ \dot{V}(e_u) = e_u \dot{e}_u = e_u(-c_2 e_u) = -c_2 e_u^2 < 0 \end{cases} \tag{11}$$

Since constant c_1 and c_2 are positive, the proposed control is asymptotically stable.

Ignore the resistance R_L, $e_i = i_q^* - i_q$ and $e_u = U_{dc}^* - U_{dc}$ are taken into (9), after simultaneous solution with equation (4) and(5),it can be got that

$$\begin{cases} \sigma_i = c_1(i_q^* - i_q) - \omega i_q + \frac{1}{L} u_d - \frac{1}{L} e_d \\ \sigma_u = c_2 e_u - \frac{S_d i_d + S_q i_q - i_{dc2}}{C} \end{cases} \tag{12}$$

Obviously, $dU_{dc}^* / dt = di_q^* / dt = 0$. The switching function of the proposed SM is as follows from equation (7), (8) and (12)

$$\begin{cases} \sigma_i = c_1(i_q^* - i_q) = 0 \\ \sigma_u = \frac{e_d}{CU_{dc}} (\frac{c_2 CU_{dc}}{e_d} e_u + \frac{U_{dc} i_{dc2}}{e_d} - i_d) = 0 \end{cases} \tag{13}$$

The two equations in (13) are divided by c_1 and e_d/CU_{dc} respectively, $c_m = c_2 CU_{dc} / e_d$ the equation can be simplified as

$$\begin{cases} \sigma_i = i_q^* - i_q = 0 \\ \sigma_u = i_d^* - i_d = 0 \end{cases} \tag{14}$$

in (14)

$$\begin{cases} i_q^* = 0 \\ i_d^* = c_m(U_{dc}^* - U_{dc}) + \frac{U_{dc} i_{dc2}}{e_d} \end{cases} \tag{15}$$

It can be seen that the model of voltage SMC controller contains only value of the output dc voltage and load current, dc side capacitor and the grid line voltage RMS e_d, so it is easy to realize digitally. The dc output of the voltage outer loop is the given current i_d^* for the inner current feedback loop.

4. Variable structure current controller based on the input output linearization

The response speed of current loop is more quickly than the voltage loop, so its current instruction i_d^* Variable structure current controller based on the input output linearization, namely the output of voltage outer loop can be considered as constant. Set $e_1 = i_d - i_d^*$, $e_2 = i_q - i_q^*$, equation (4) can be turned into

$$\frac{d}{dx}\begin{bmatrix} e_1 \\ e_2 \end{bmatrix} = \begin{bmatrix} -\frac{R_L}{L}e_1 - \frac{R_L}{L}i_d^* + \omega i_q + \frac{e_d}{L} - \frac{u_d}{L} \\ -\frac{R_L}{L}e_2 - \frac{R_L}{L}i_q^* - \omega i_d - \frac{u_q}{L} \end{bmatrix} \tag{16}$$

When not to consider system disturbance, the equation (16) can be expressed as the two input two output affine nonlinear models

$$\begin{cases} \dot{x} = f(x) + G(x)u \\ y_1 = h_1(x) \\ y_2 = h_2(x) \end{cases} \tag{17}$$

Where

$$f(x) = \begin{bmatrix} -\frac{R_L}{L}e_1 - \frac{R_L}{L}i_d^* + \omega i_q + \frac{e_d}{L} \\ -\frac{R_L}{L}e_2 - \frac{R_L}{L}i_q^* - \omega i_d \end{bmatrix}, \quad G(x) = \begin{bmatrix} -\frac{1}{L} & 0 \\ 0 & -\frac{1}{L} \end{bmatrix}$$

$x = [x_1, x_2] = [e_1, e_2] = [i_d - i_d^*, i_q - i_q^*]$, $u = [u_d, u_q]$, $y = [y_1, y_2] = h(x) = [h_1(x), h_2(x)] = [e_1, e_2]$。

Affine nonlinear system shown in (17) meets the exact linearization condition. System vector relative degree $r = [r_1, r_2] = [1,1]$, Lie derivative of the function *h* to the function *G* is

$$L_g h(x) = \frac{\partial h(x)}{\partial x} G(x) = \begin{bmatrix} 1 & 0 \\ 0 & 1 \end{bmatrix} \begin{bmatrix} -\frac{1}{L} & 0 \\ 0 & -\frac{1}{L} \end{bmatrix} = \begin{bmatrix} -\frac{1}{L} & 0 \\ 0 & -\frac{1}{L} \end{bmatrix} \tag{18}$$

Defining a $m \times m$ matrix, $A(x)$

$$A(x) = \begin{bmatrix} L_{g_1}\left(L_f^{r_1-1}h_j\right) & \cdots & L_{g_m}\left(L_f^{r_1-1}h_j\right) \\ \vdots & \ddots & \vdots \\ L_{g_1}\left(L_f^{r_m-1}h_m\right) & \cdots & L_{g_m}\left(L_f^{r_m-1}h_m\right) \end{bmatrix} = \begin{bmatrix} -\frac{1}{L} & 0 \\ 0 & -\frac{1}{L} \end{bmatrix} \tag{19}$$

The Lie derivative of $h(x)$ to function $f, L_f h_1$ and $L_f h_2$ are shown in (20) and (21)

$$L_f h_1 = \frac{\partial h_1(x)}{\partial x} f(x) = \begin{bmatrix} 1 & 0 \end{bmatrix} \begin{bmatrix} -\frac{R_L}{L}e_1 - \frac{R_L}{L}i_d^* + \omega i_q + \frac{e_d}{L} \\ -\frac{R_L}{L}e_2 - \frac{R_L}{L}i_q^* - \omega i_d \end{bmatrix} = -\frac{R_L}{L}e_1 - \frac{R_L}{L}i_d^* + \omega i_q + \frac{e_d}{L} \tag{20}$$

$$L_f h_2 = \frac{\partial h_2(x)}{\partial x} f(x) = \begin{bmatrix} 0 & 1 \end{bmatrix} \begin{bmatrix} -\frac{R_L}{L}e_1 - \frac{R_L}{L}i_d^* + \omega i_q + \frac{e_d}{L} \\ -\frac{R_L}{L}e_2 - \frac{R_L}{L}i_q^* - \omega i_d \end{bmatrix} = -\frac{R_L}{L}e_2 - \frac{R_L}{L}i_q^* - \omega i_d \tag{21}$$

The system output derivatives of time can be expressed as:

$$\begin{bmatrix} \dot{y}_1 \\ \dot{y}_2 \end{bmatrix} = \begin{bmatrix} L_f h_1 \\ L_f h_2 \end{bmatrix} + A(x) \begin{bmatrix} u_1 \\ u_2 \end{bmatrix} \tag{22}$$

Obviously $A(x)$ is reversible, the feedback control law can be express as

$$u = -A^{-1}(x) \begin{bmatrix} L_f h_1 \\ L_f h_2 \end{bmatrix} + A^{-1}(x) v \tag{23}$$

The available input/output dynamic equations is

$$\begin{bmatrix} \dot{y}_1 \\ \dot{y}_2 \end{bmatrix} = v = \begin{bmatrix} v_1 \\ v_2 \end{bmatrix} \tag{24}$$

Comprehensive formula (4) (23) (40) are

$$\begin{cases} u_d = -R_L e_1 - R_L i_d^* + \omega L i_q + e_d - L v_1 \\ u_q = -R_L e_2 - R_L i_q^* - \omega L i_d - L v_2 \end{cases} \tag{25}$$

Take $v = [v_1, v_2] = [k_1 y_1, k_2 y_2] = [k_1 e_1, k_2 e_2]$, then the above equation can be translated into

$$\begin{cases} u_d = -(R_L + k_1 L) e_1 - R_L i_d^* + \omega L i_q + e_d \\ u_q = -(R_L + k_2 L) e_2 - R_L i_q^* - \omega L i_d \end{cases} \tag{26}$$

Select the appropriate feedback coefficient k_1,k_2 can obtain good dynamic and static performance. When the relative order of the uncertain disturbance system is lower than that of the system without perturbation, the zero dynamics of the system may become unstable due to disturbances. In order to reduce the possibility, when current loop controller is designed, variable structure control added into the input-output linearization above mentioned to enhance the anti-interference ability.

$$\dot{x} = f(x) + G(x)u + d(t, x) \tag{27}$$

where $d(t, x)$ is a uncertain perturbation.

Assuming uncertain disturbance $d(t, x)$ is within the scope of control, let $s = s(x)$ is a sliding surface, the following variable structure controller is designed

$$u = -(\frac{\partial s}{\partial x} G)^{-1} (\frac{\partial s}{\partial x} f + \lambda s + \mu \operatorname{sgn}(s)) \tag{28}$$

Where $\lambda \geq 0$, $\mu > 0$ are to be determined, and $\frac{\partial s}{\partial x} G$ is reversible. A corresponding nonlinear state transformation is as follows

$$z_i^j = T_i^j(x) = L_f^j h_i, i = 1, \cdots, m; j = 0, 1, \cdots, r_i - 1 \tag{29}$$

Namely

$$\begin{cases} z_1 = T_1(x) = L_f^0 h_1 = e_1 \\ z_2 = T_2(x) = L_f^0 h_2 = e_2 \end{cases} \tag{30}$$

then

$$z = y = [e_1, e_2]^T \tag{31}$$

Then the switching function of $s = s(x)$ can be expressed as

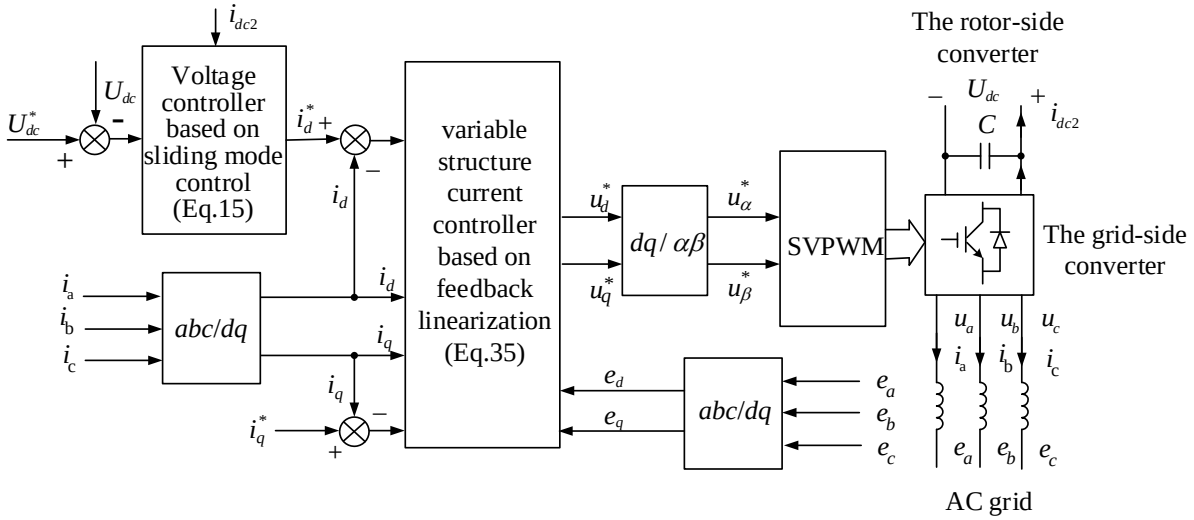

Figure 3. The dual-loop control diagram with sliding mode control in outer voltage loop and linearization variable structure control in inner current loop

$$s_i(z_i) = z_i \tag{32}$$

Namely
$$s(x) = z = \left[e_1, e_2\right]^T \tag{33}$$

Combination (28) with (33) can get control law

$$\begin{aligned} u &= -(\frac{\partial s}{\partial x}G)^{-1}(\frac{\partial s}{\partial x}f + \lambda s + \mu \mathrm{sgn}(s)) \\ &= -\begin{bmatrix} -L & 0 \\ 0 & -L \end{bmatrix}\left(\begin{bmatrix} -\frac{R_L}{L}e_1 - \frac{R_L}{L}i_d^* + \omega i_q + \frac{e_d}{L} \\ -\frac{R_L}{L}e_2 - \frac{R_L}{L}i_q^* - \omega i_d \end{bmatrix} + \begin{bmatrix} \lambda_1 e_1 \\ \lambda_2 e_2 \end{bmatrix} + \begin{bmatrix} \mu_1 \mathrm{sgn}(e_1) \\ \mu_2 \mathrm{sgn}(e_2) \end{bmatrix}\right) \end{aligned} \tag{34}$$

$$\begin{cases} u_d = (\lambda_1 L - R_L)e_1 + \mu_1 L \mathrm{sgn}(e_1) - R_L i_d^* + \omega L i_q + e_d \\ u_q = (\lambda_2 L - R_L)e_2 + \mu_1 L \mathrm{sgn}(e_1) - R_L i_q^* - \omega L i_d \end{cases} \tag{35}$$

Setting $[m_1, m_2] = [\lambda_1 L - R_L, \lambda_1 L - R_L]$ and then calculating the appropriate m_1, m_2, μ_1 and μ_2 assure of good static and dynamic performance. After u_d, u_q have gotten, transforming them into α-β axis, control single can be gotten by using SVPWM modulation .The overall control block diagram is shown in Figure 3.

5. Simulation

The proposed control system presented in figure 3 has been simulating evaluated by using a prototype shown in figure 1. The grid-side converter is connected to the AC grid by using input filter inductors L = 5.0mH with R_L=0.02 Ω . The dc link is composed by capacitors of 2200 μF with a reference voltage of 300V. In the voltage sliding mode control controller module based on the formula (15), the coefficient c_m=1, as well as in the current controller according to formula (35), the coefficient m_1 =m_2 = 50, μ_1 = 50, μ_2 = 25.The rms value of AC side voltage is110V with frequency of 50Hz. The resistance R_L = 0.02, L = 5mH, switching frequency for power devices is 10 kHz, the rotor-side convert is instead by a resistance of 50Ω on DC side.

Figure 4 shows the simulation waveforms under different conditions. It can be seen that from figure 4 (a), the overshoot of dc voltage is 5%, with voltage peak of 315V. It reaches 300V in 0.03 seconds

and then maintains stability. When the reference voltage suddenly increased from 300V to 400V at 0.1 seconds, as shown in figure 4 (c), the dc voltage dropped off about 15V at firstly. After 0.009 seconds, it reaches steady 400V without overshoot. If the dc load reduced to its half at 0.1 seconds, as shown in figure 4(e), a 1V voltage jump happened on dc side and back to the steady-state value of 300V after 0.02 seconds. If dc voltage of 400V generated by an inverter add to the dc side at 0.1 seconds, as shown in figure 4 (g), it can be seen that dc voltage return its steady state after 0.03 seconds. The simulation result approves that the control strategy this paper proposed has good dynamic characteristics and robustness.

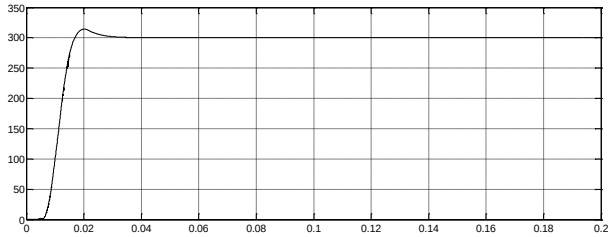

Figure 4. (a) dc voltage waveform

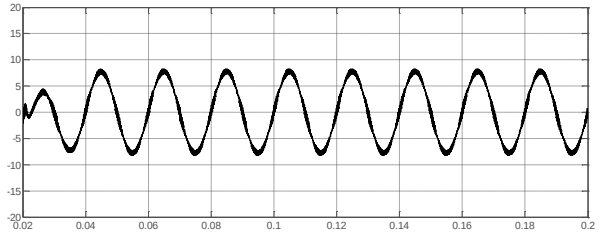

Figure 4. (b) a phase current waveform on ac side

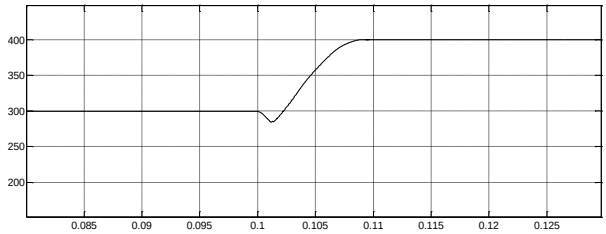

Figure 4. (c) DC voltage waveform when dc reference voltage changed suddenly

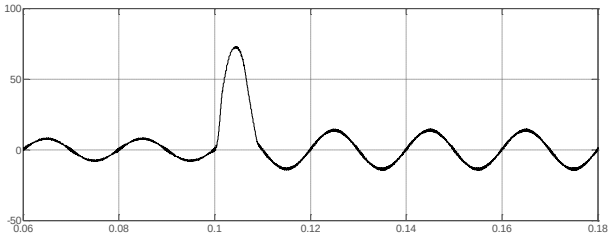

Figure 4. (d) A phase current waveform on ac side when dc reference voltage changed suddenly

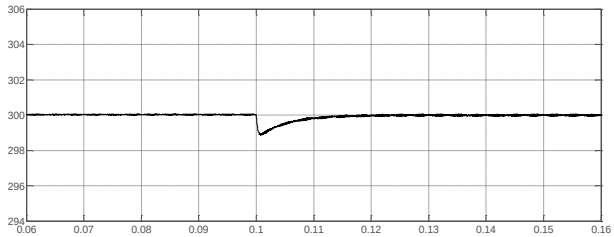

Figure 4. (e) DC voltage waveform when the load reduced to its half

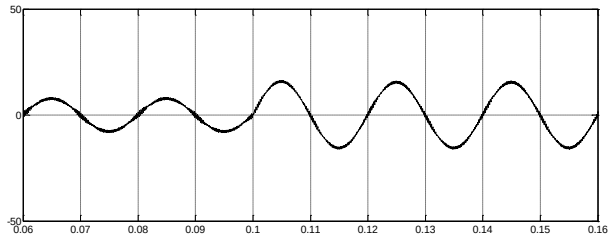

Figure 4. (f) A phase current waveform on ac side when the load reduced to its half

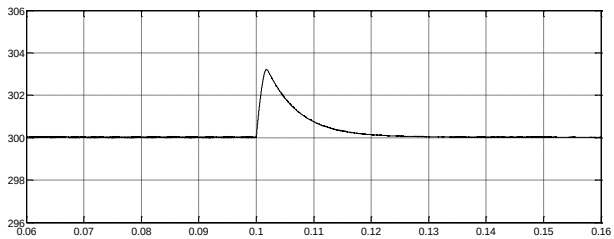

Figure 4. (g) dc voltage waveform when dc voltage source 400V added on dc side

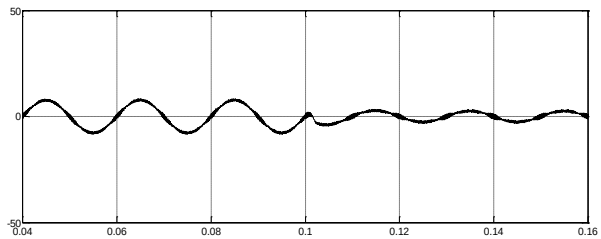

Figure 4. (h) A phase current waveform on ac side when dc voltage source of 400V added on dc side

Figure 4. Simulation waveforms under different conditions

6. Conclusion

This paper has proposed a control approach for improving the performance of the grid side converter in a doubly-fed induction generator used in the wind power system. In this control approach, the

dcvoltage is regulated by a sliding mode variable structure control scheme and current by a variable structure controller based on the input output linearization. The theoretical bases of the sliding mode variable structure control was introduced, and the stability proof was presented. Switching function of the system has been deduced, sliding mode voltage controller model has been established, and the output of the outer voltage loop is the instruction of the inner current loop. Affine nonlinear model of two input two output equations on d-q axis for current has been established, its meeting conditions of exact linearization were proved. In order to improve the anti-jamming capability of the system, a variable structure control was added in the current controller, the control law was deduced. The dual-loop control diagram with sliding mode control in outer voltage loop and linearization variable structure control in inner current loop was proposed. Simulation results demonstrates the effectiveness of the proposed control strategy even during the dc reference voltage and system load variation.

Acknowledgments
The research work was supported by the Natural Science Foundation of Hubei Province, China, No. 2012FFB6413

References
[1] Ren J, Wang J , Hu Y and Ji Y 2014 *Electric Power Automation Equipment* **34** 108-13
[2] Song H and Qu Y 2012 *J. Control Theory and Applications* **10** 435-40
[3] Shao Z L, Shi M Q, Han Z F, Wang X D and Li Q M 2014 *Applied Decisions in Area of Mechanical Engineering and Industrial Manufacturing* **577** 321-4
[4] Tang H, Zhao R X, Tang S Q and Zeng Z 2012 *Ieee International Symposium on Industrial Electronics* 270-4
[5] Patnaik R K and Dash P K 2016 *IET Renewable Power Generation* **10** 598-610
[6] Shen Y, Zhang L, Chen H, Lu X F and Qian Z 2014 *26th Chinese Control and Decision Conference*(CCDC2014) 991-3
[7] Zhang Y C, Zhang Q, Li Z X and Zhang Y C 2013 *International Conference on Electrical Machines and Systems* 2207-12
[8] Chen W, Geng X J, Liu T and Xia C L 2014 *Electric Power Systems Research***108** 223-33
[9] Gao J L, Zheng T Q and Lin F 2011 *J. Power Electronics* **11** 64-73
[10] Setiawan I, Priyadi A, Miyauchi H and Purnomo M H 2015 *Ieej Transactions on Electrical and Electronic Engineering* **10** 674-82
[11] Wang C and Zhou J 2015 *Proc. Chinese Automation Congress*(CAC2015) 1252-7